Indian Journal of Chemistry
Vol. 52A, December 2013, pp. 1570-1575

Mechanochemical synthesis of nanohydroxyapatite bioceramics

Sharifah Adzila[a, b], Iis Sopyan[c], Tan Chou Yong[a], Ramesh Singh[a, *], Wong Yew Hoong[a], J Purbolaksono[a] & Mohd. Hamdi[a]

[a]Centre of Advanced Manufacturing and Material Processing, Department of Mechanical Engineering, Faculty of Engineering, University of Malaya, 50603 Kuala Lumpur, Malaysia

Email: ramesh79@um.edu.my

[b]Department of Materials Engineering and Design, Faculty of Mechanical and Manufacturing Engineering, University of Tun Hussein Onn Malaysia, 86400 Johor, Malaysia

[c]Department of Manufacturing and Materials Engineering, Faculty of Engineering, International Islamic University Malaysia, 50728 Kuala Lumpur, Malaysia

Received 12 April 2013; revised and accepted 19 November 2013

Nanosized hydroxyapatite powder has been synthesized by the mechanochemical method using a dry mixture of calcium hydroxide and diammonium hydrogen phosphate. The effect of mechanochemical process on powder properties has been investigated. Three rotation speeds of 170 rpm, 270 rpm and 370 rpm have been employed with 15 hours milling time. Characterization of the nanopowders has been accomplished by Fourier transform infra red, X-ray diffraction and transmission electron microscopy analyses. The samples have been prepared and sintered in air at varying temperatures ranging from 1050–1350 °C. Results show that increase in rotation speed (370 rpm) increases the crystallite size (9–21 nm). Agglomerate formation with irregular shapes is found in the samples prepared at 270 and 370 rpm. The sintering process influences the stability of powder by yielding TCP phase at all the sintering temperatures. At 370 rpm, the sample sintered at 1250 °C shows the maximum relative density of 95.3% as well as hardness of 5.3 GPa.

Keywords: Mechanochemical synthesis, Nanomaterials, Hydroxyapatite, Bioceramics

Hydroxyapatite (HA) is commonly used for a number of biomedical applications in the forms of granules, blocks[1], coatings and dense bodies[1-5] for bone augmentation. HA has also been found useful for drug delivery and antibiotics[6]. It exists naturally in human bone as crystals within collagen. The high strength is necessary for reliable implant in the body[7]. Many improvements have been made to overcome the limitation of HA in loading application by controlling microstructures via novel sintering techniques or utilization of nanopowders[8]. Development of dense HA ceramics with superior mechanical properties is possible if the starting powder is stoichiometric with improved powder properties such as crystallinity, agglomeration and morphology[1-3]. Nanoscale grain size in dense sintered materials is a desired parameter to enhance the mechanical and biological properties of HA-based bioceramic materials[9]. Several methods have been applied for synthesizing HA nanocrystalline powder like wet precipitation[10], sol-gel[11], hydrothermal[12] and mechanochemical[13].

Mechanochemical ball milling has been used since 1922 wherein the materials components are synthesized by deformation process through ball-particle, particle-wall, and particle-particle collisions[14] at a particular time, leading to the chemical reaction between particles to form new nanosize composites or powders. It is a simple and low cost method compared to other techniques, and has recently received attention as an alternative route in preparing materials characterized by better biocompatibility with natural bone[13]. Synthesis of HA through mechanochemical milling can be in either a wet medium[15] or under dry condition[13]. The dry mechanochemical method is reported to be more beneficial than the wet mechanochemical method due to faster reactions in absence of water. In addition, the dry condition provides a lower level of contamination by the mill material[16], whereby powders obtained can be used directly without filtering and drying[16] stage, as compared to under wet conditions. Some studies have used dry mechanochemical method in producing calcium phosphate bioceramics under various milling times[13], fluoride substituted HA[17] and nanocomposite HA[18]. In this work the properties of HA prepared via the mechanochemical method was investigated.

Materials and Methods

Synthesis of the hydroxyapatite (HA) powder

Commercially available calcium hydroxide ($Ca(OH)_2$) and diammonium hydrogen phosphate [$(NH_4)_2HPO_4$] purchased from R&M Chemicals (UK) and Systerm Sdn. Bhd. (Malaysia) respectively were use as the precursors.

The mixed precursors with molar ratio of 1.67 Ca/P were milled by using tungsten carbide vials and balls as milling medium in the Fritsch planetary ball mill. The powder to ball mass ratio was 1/6. The three rotation speeds; 170 rpm, 270 rpm and 370 rpm were employed for 15 hours of milling. The interval pause was set for 1 hour after every 1 hour milling time. The reaction of the two precursors is described in Eq. 1.

$$5Ca(OH)_2 + 3(NH_4)_2HPO_4 \rightarrow Ca_5(PO_4)_3OH + 6NH_3 + 9H_2O \quad \ldots(1)$$

The as-synthesized powders were uniaxially pressed into pellet form in a steel die of 10.5 mm in diameter under 2.5 MPa loading, followed by cold isostatic pressed (CIP) at 200 MPa for 5 min. These green bodies were sintered for 2 h at different temperatures, i.e., 1050 °C, 1150 °C, 1250 °C and 1350 °C, under air atmosphere with heating and cooling rates at 5 °C/min.

Characterisation of the hydroxyapatite powder

The phase existence in the as-synthesized powders and the sintered compacts were identified using an X-ray diffractometer (Cu-Kα, Shimadzu XRD 6000 diffractometer). All measurements were performed at room temperature in the range of 2θ = 25–42° at 2°/min scan speed. The phase existence was compared to the standards of the Joint Committee of Powder Diffraction Standards (JCPDS) card number; 09-0432 for HA phase, 09-0169 for β-TCP phase and 29-0359 for α-TCP phase. The average crystallite size (***D***) of the as-synthesized powders was calculated by using Scherrer's equation[19], $\boldsymbol{D} = K / \sin$, where K is the shape factor equal to 0.9, λ is the X-ray wavelength (equal to 1.5406 Å for Cu-K radiation), θ is the Bragg's diffraction angle (in degrees), β is the full-width at half-maximum (FWHM)[20]. The degree of crystallinity (Xc)[21] was calculated through using the equation, $Xc = 1 - \boldsymbol{V}_{112/300} / \boldsymbol{I}_{300}$, where $\boldsymbol{I}_{300}$ is the intensity of (300) reflection of HA and $\boldsymbol{V}_{112/300}$ is the intensity of the hollow between (112) and (300) reflections[22]. The lattice constants of the as-synthesized powders were determined and the volume of the hexagonal unit cell of the materials was calculated according to the formula[21], $\boldsymbol{V} = 2.589\ (\boldsymbol{a}^2)\boldsymbol{c}$, where $\boldsymbol{V}$ (Å^3) is the volume of unit cell, $\boldsymbol{a}$ and $\boldsymbol{c}$ are the hexagonal lattice constants in Angstrom. The functional group of the as-synthesized powders was analyzed using Perkin-Elmer Spectrum FTIR spectrometer in the range of 4000–380 cm^{-1} with 4 cm^{-1} resolution. The particle size and shape of the powders were examined under transmission electron microscope (Philips HMG 400 TEM) after 30 minutes sonication of the powder suspension in ethanol solution.

The relative density of the sintered bodies was measured by Archimedes' method by taking the theoretical density of HA[23] as 3.156 g cm^{-3}. The sintered samples were ground and polished to 1 μm finish. Vickers microhardness test was carried out using MVK H2 hardness tester with 200 g f load and the samples were subsequently gold coated prior to scanning electron microscopy analysis.

Results and Discussion

IR spectra

The chemical functionality of the as-synthesized HA was determined by Fourier transform infrared (FTIR) analysis. Figure 1 shows the IR spectra of the as-synthesized powders with various rotation speeds from 170-370 rpm. Phosphate (PO_4) band has four vibration modes, ν_1, ν_2, ν_3, and ν_4. The samples in all the rotation speeds show the PO_4 band at around 962 cm^{-1} (ν_1) and 474 cm^{-1} (ν_2). Besides, the bands for PO_4 are observed at around 1088 cm^{-1} (ν_3), 1023 cm^{-1}(ν_3), 599 cm^{-1} (ν_4) and 560 cm^{-1} (ν_4). The weak vibration band at 628 cm^{-1} corresponds to OH group and can be seen prominently when the rotation

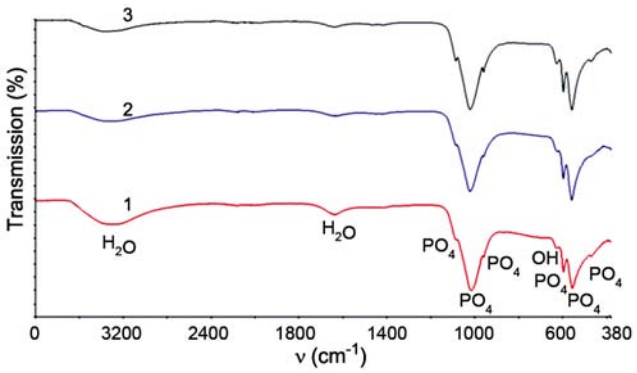

Fig. 1 – IR spectra for various rotation speeds of mechanochemically synthesized powders. [(1) 170 rpm; (2) 270 rpm; (3) 370 rpm].

Table 1 – Unit cell parameters of HA reference standard and the as-synthesised samples at various rotation speeds

Sample	***a***-Axis (Å)	***c***-Axis (Å)	***V*** (Å^3)
HA (09-432)	9.4600	6.8800	1594.05
170 rpm	9.4648	6.8748	1594.47
270 rpm	9.4547	6.8997	1596.83
370 rpm	9.4479	6.8919	1592.73

speed was increased to 370 rpm. The broad band in the range of 3200–3600 cm^{-1} is ascribed to the absorbed moisture (H_2O). The existence of phosphate and hydroxyl groups indicate that HA is produced by milling in all the rotation speeds employed.

Crystallite size

The crystallite size was calculated using the Scherrer's equation[15,19]. For this purpose, FWHM at (300) (2θ = 25.8°) has been chosen to calculate the crystallite size. The crystallite size increased from 9.4 nm (170 rpm) to 11.4 nm (270 rpm) and subsequently to 21 nm (370 rpm)[1]. The findings correspond well with earlier work reported by Silva ***et al***.[19], who observed that the degree of crystallinity increased linearly with the rotation speed. In comparison, the crystallite size (21 nm) obtained at 370 rpm for the current work is higher than that reported by Silva ***et al***.[19] (14.3 nm) with $Ca(CO)_3$ and $CaH(PO)_4$ as precursors and lower than crystallite size obtained from $CaCO_3$ and $(HN_4)H_2PO_4$ precursors (35.5 nm). Increased rotation speed led to the production of increased crystallite size and maximum crystallinity degree. Table 1 shows the hexagonal unit cell parameters consist of ***a*** and ***c*** axes and the unit cell volume. HA from the reference standard has the ***a*** axis = 9.4600 Å, ***c*** axis = 6.8800 Å and unit cell volume = 1594.05 Å^3. Of the three samples, only that produced at 170 rpm possesses unit cell parameters similar to that of the HA reference standard.

From the TEM analysis (Fig. 2), powder size ranging from 43–55 nm was found in samples synthesized at 170 rpm rotation speed (Fig. 2a). The powder size was further reduced as the speed was increased to 270 and 370 rpm (9–31 nm, Figs 2b and 2c). Spherical shapes were obtained at 170 rpm speed while powders synthesized using 270 and 370 rpm speed consist of irregular shapes (rod and spherical shapes). The obvious hard agglomeration formation was observed in sample subjected to 270 rpm speed (Fig. 2b). This phenomenon may also

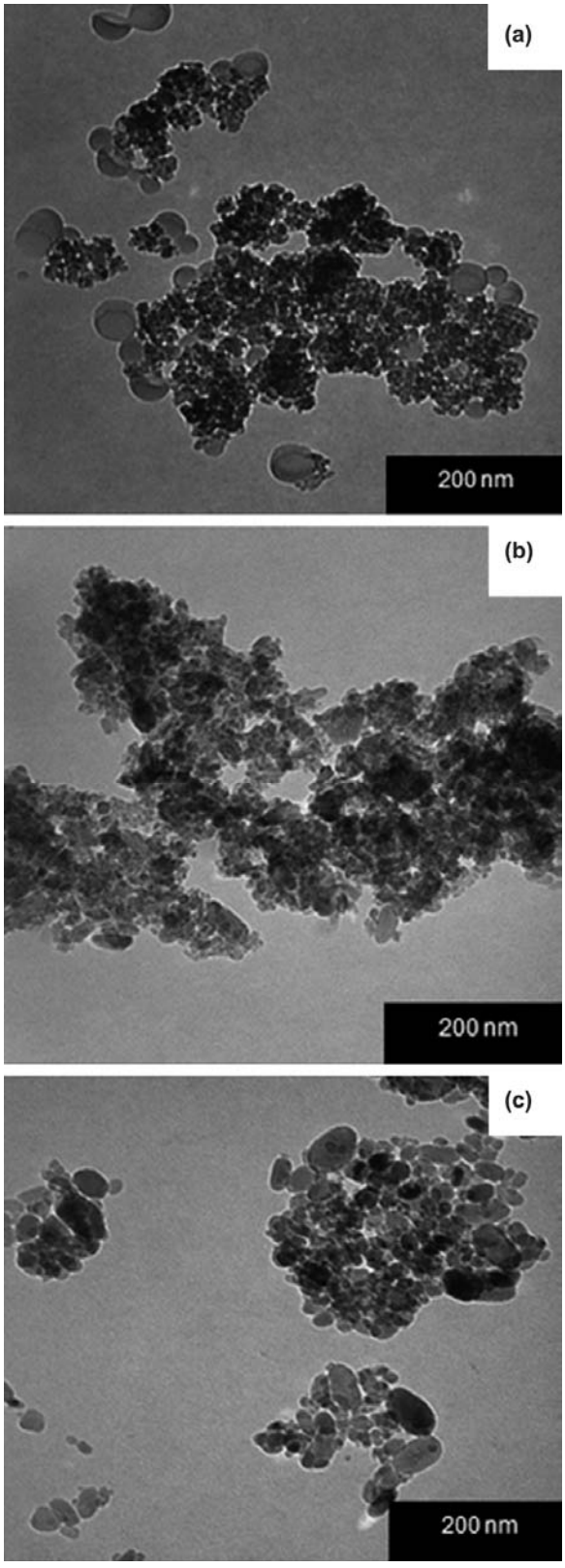

Fig. 2 – Microstructure of the mechanochemically synthesized powders at varying rotation speeds. [(a) 170 rpm; (b) 270 rpm; (c) 370 rpm].

be due to the fact that as the speed increases, the balls movement will increase with increase in kinetic energy leading to increased impact from collision between balls and vial wall which is transferred to the particles. The high energy will break them into smaller fragments, thus reducing the particle sizes to the nanoscale range.

Microhardness and density

The 1250 °C sintered compacts for the milled powders at the three different speeds were subjected to Vickers microhardness test and density measurement by the Archimedes method. Results show that with increase in rotation speed, the hardness increased linearly (4.14–5.30 GPa) as also the relative density[1] (92.6 to 95.3%). From these results, it can be seen that the increase in hardness is related to the relative density. This relationship could also be affected by particle size where smaller particle size generally increases the specific surface area as well as the driving force for densification leading to higher mechanical properties[24]. Hence, higher density and higher hardness are controlled by the bonding amongst the grains in the sintered samples[25].

The XRD patterns of the 1250 °C sintered compacts for powders milled at 170 rpm show that the HA phase is present along with β-TCP (beta-tricalcium phosphate), α-TCP (alpha-tricalcium phosphate) and TTCP (tetratricalcium phosphate) phases (Fig. 3). As the speed was increased to 270 rpm, the intensity of the peaks of the HA and α-TCP was observed to decrease slightly. This was followed by an increase in the β-TCP intensity. In contrast, the 370 rpm powders exhibited the HA and β-TCP phases.

The fraction of the HA and secondary phases measured for the sintered (1250 °C) samples is shown in Table 2. The results show that the fraction of HA phase decreases from 71.5 to 56.8% with increase in rotation speed from 170 to 370 rpm. In contrast, the fraction of β-TCP phase increases from 14.5 to 43.2% as the rotation speed increases to 370 rpm. The α-TCP phase (13.9%) was only found for the sample prepared at 170 rpm rotation speed. This sample also recorded the lowest hardness when compared to the 270 and 370 rpm samples. The decomposition of the HA phase is due to the formation of an intermediate phase, oxyapatite, that is formed by the gradual loss of the radical OH^- (dehydroxylation) when heated under atmospheric condition[26]. Thus, HA is prone to release H_2O during the heating process, leading to TCP and pore formation.

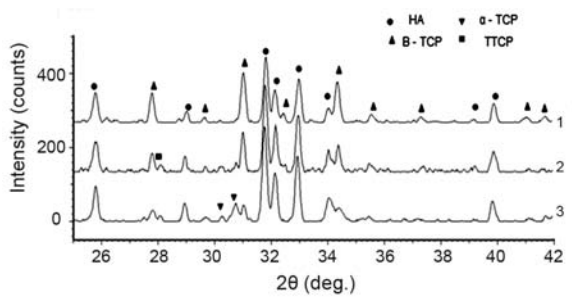

Fig. 3 – XRD pattern of 1250 °C sintered compacts milled at varying rotation speeds. [(1) 170 rpm; (2) 270 rpm; (3) 370 rpm].

Linear shrinkage, hardness and relative density have been studied as a function of sintering temperature from 1050–1350 °C for 370 rpm sintered compacts (Table 3). The results show that hardness and relative density increase linearly until 1250 °C (1.2–5.3 GPa, 89.0–95.3%)[1] and finally decrease at 1350 °C (3.46 GPa, 90.6%). In contrast, linear shrinkage is proportional with sintering temperatures and increases until 1350 °C (7.3–17.3%). The decrease of relative density and hardness may be associated with the decomposition of the HA phase at higher temperature whereby the secondary phases may obstruct the bonding between the HA grains[25], thus resulting in poor densification and mechanical properties. In addition, the mechanical properties of ceramics can be influence by the grain size[27] and has been reported to decrease when the grain size exceeded some critical limit[23].

Table 2 – The phases present after sintering at 1250 °C at varying rotation speeds

Rotation speed (rpm)	Phase comp. (%)		
	HA	β-TCP	α-TCP
170	71.5	14.5	13.9
270	67.7	32.3	-
370	56.8	43.2	-

Table 3 – Properties of compacts (powder prepared at 370 rpm rotation speed) sintered at varying temperatures

Sintering temp. (ºC)	Vickers hardness (GPa)	Relative density (%)	Linear shrinkage (%)
1050	1.20	89.0	7.3
1150	3.11	90.0	11.2
1250	5.30	95.3	13.1
1350	3.46	90.6	17.3

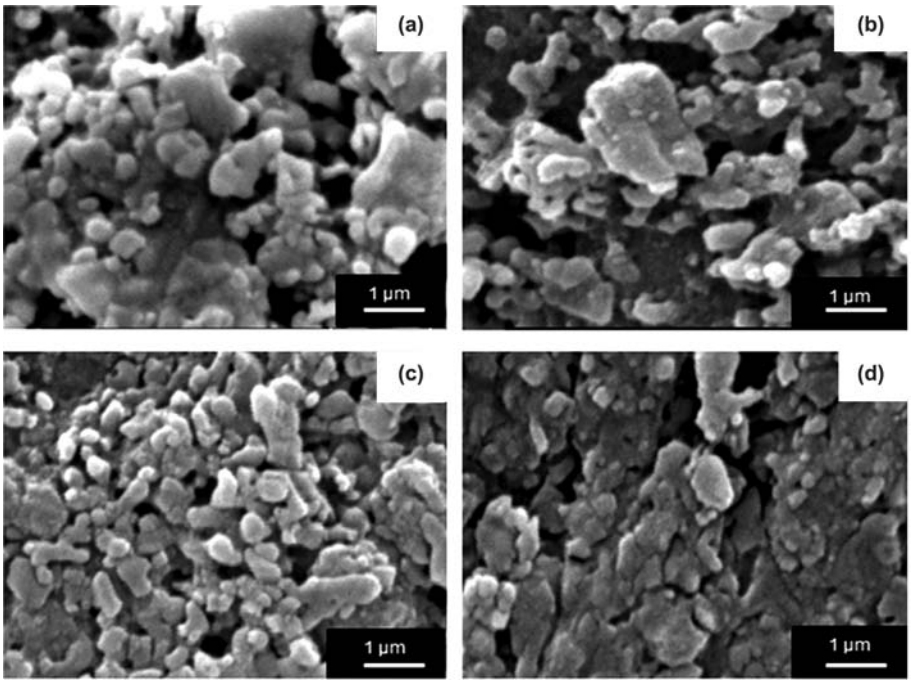

Fig. 4 – Microstructure of samples sintered at 1250 and 1350 °C. [Temp.: 1250 °C; (a) 170 rpm; (b) 270 rpm; (c) 370 rpm. Temp.: 1350 °C; (d) 370 rpm].

Microstructure of the hydroxyapatite powders

The microstructure evolution of the sintered samples obtained at 1250 °C and 1350 °C for the samples prepared at different rotation speed are presented in Fig. 4. At 1250 °C, the coalescence particles can be seen in 170 rpm powders (Fig. 4a), where the grain boundaries are diffused and porosity reduced to form larger grains. This occurs also in the 270 rpm compacts as shown in Fig. 4(b). The necking process occurs where smaller grain is observed in 370 rpm powders (Fig. 4c).

At 1350 °C, the grain growth becomes more pronounced for the 370 rpm powder with less porosity (Fig. 4d). The pores and heating condition are the main factors in the densification process where higher temperature reduces the porosity and increases the density, which increases the hardness until the optimum sintering temperature has been reached. On the other hand, when the temperature increases, grain coarsening and pore elimination will occur and this could possibly reduce the hardness[28]. This is evident for sintering at 1350 °C wherein the samples exhibited lower hardness (3.46 GPa) and lower relative density (90.6%).

Conclusions

Nanocrystalline hydroxyapatite powder has been successfully synthesized through dry mechanochemical method milled at varying rotation speeds of 170, 270 and 370 rpm. FTIR and XRD analyses confirm the formation of HA. In the current study, 370 rpm is found to be the optimum rotation speed for HA synthesis since it increases the crystallite size and crystallinity degree of the synthesized powders. TEM analysis shows that the powder consists of irregular shapes ranging from sphere-like to rod-like shape. Decrease of particle size is observed as the speed is increased to 270 and 370 rpm. The maximum hardness of 5.30 GPa and relative density of 95.3% is found in powders milled at 370 rpm when sintered at 1250 °C. At similar temperature, the β-TCP, α-TCP and TTCP phases are observed in powders prepared at 170 and 270 rpm. However, at 370 rpm, only β-TCP has been detected along with the HA phase. In addition, at 370 rpm rotation speed, the particle size of the powder decreases and on sintering at 1250 °C resulted in finer grain sizes which leads to maximum hardness and relative density.

Acknowledgement

This study was supported under the HIR grant (No. H-16001-00-D000027). The authors thank Biomedical Engineering Research Group of International Islamic University Malaysia (IIUM), Malaysia and Institute of Research Management and Monitoring (IPPP) of University of Malaya, Malaysia for supporting this research.

References

1 Adzila S, Sopyan I, Hamdi M & Ramesh S, ***Mater Sci Forum***, 694 (2011) 118.
2 Sopyan I, Mel M, Ramesh S & Khalid K A, ***Sci Tech Adv Mater***, 8 (2007) 116.
3 Sopyan I & Kaur J, ***Ceram Int***, 35 (2009) 3161.
4 Toque J A, Herliansyah M K, Hamdi M, Ektessabi A I & Sopyan I, ***J Mech Behav Biomed Mater***, 3 (2010) 324.
5 Sopyan I & Natasha A N, ***Ionics*** 12 (2009) 735.
6 Wang S, Wang X, Xu H, Abe H, Tan Z, Zhao Y, Guo J, Naito M, Ichikawa H & Fukumori Y, ***Adv Powd Tech***, 21 (2010) 268.
7 Webster T J, Massa-Schlueter E A, Smith J L & Slamovich E B, ***Biomaterials***, 25 (2004) 2111.
8 Wang J & Shaw L L, ***Biomaterials***, 30 (2009) 6565.
9 Tang C Y, Uskokovic P S, Tsui C P, Veljovic D, Petrovic R & Janackovic D, ***Ceram Int***, 35 (2009) 2171.
10 Ramesh S, Tan C Y, Bhaduri S B, Teng W D & Sopyan I, ***J Mater Proc Tech,*** 206 (2008) 221.
11 Sopyan I, Ramesh S & Hamdi M, ***Indian J Chem***, 47A (2008) 1626.
12 Alqap A S F & Sopyan I, ***Indian J Chem***, 48A (2009) 1492.
13 Nasiri-Tabrizi B, Honarmandi P, Ebrahimi-Kahrizsangi R & Honarmandi P, ***Mater Lett***, 63 (2009) 543.
14 Karlinsey R & Mackey A, ***J Mater Sci***, 44 (2009) 346.
15 Mostafa N Y, ***Mater Chem & Phy,*** 94 (2005) 333.
16 El Briak-Ben Abdeslam H, Ginebra M P, Vert M, Boudeville P, ***Act Biomaterialia*** 4 (2008) 378.
17 Zahrani E M & Fathi M H, ***Ceram Int***, 35 (2009) 2311.
18 Fahami A R, Kahrizsangi E & Nasiri-Tabrizi B, ***Sol State Sci***, 13 (2011) 135.
19 Silva C C, Pinheiro A G, Miranda M A R, Góes J C & Sombra A S B, ***Sol State Sci***, 5 (2003) 553.
20 Ilaria C, Alessandra B, Mariangela L & Laura M, ***J Euro Ceram Soc***, 29 (2009) 2969.
21 Basar B, Tezcaner A, Keskin D & Evis Z, ***Ceram Int***, 36 (2010) 1633.
22 Hanifi A, Fathi M, Mir Mohammad Sadeghi H & Varshosaz J, ***J Mater Sci: Mater Med***, (2010) 2393.
23 Muralithran G & Ramesh S, ***Ceram Int***, 26 (2000) 221**.**
24 Song J, Liu Y, Zhang Y & Jiao L, ***Mater Sci Eng: A***, 528 (2011) 5421.
25 Gu Y W, Loha N H, Khora K A, Tora S B & Cheang P, ***Biomaterials***, 23 (2002) 2337.
26 Sanosh K P, Chu M C, Balakrishnan A, Kim T & Cho S J, ***Met Mater Int***, 16 (2010) 605.
27 Que W, Khor K A, Xu J L, & Yu L G, ***J Eur Ceram Soc***, 28 (2008) 3083.
28 Landi E A T, Celotti G & Sprio S, ***J Eur Ceram Soc***, 20 (2000) 2377.